Spinal Cord Vascular Disease: Characterization with Fast Three-Dimensional Contrast-Enhanced MR Angiography

Christoph A. Binkert, Spyros S. Kollias and Anton Valavanis

AJNR Am J Neuroradiol 1999, 20 (10) 1785-1793
http://www.ajnr.org/content/20/10/1785

AJNR Am J Neuroradiol 20:1785–1793, November/December 1999

Spinal Cord Vascular Disease: Characterization with Fast Three-Dimensional Contrast-Enhanced MR Angiography

Christoph A. Binkert, Spyros S. Kollias, and Anton Valavanis

BACKGROUND AND PURPOSE: **Noninvasive characterization of spinal vascular lesions is essential for guiding clinical management, and several MR angiographic techniques have been applied in the past with variable results. The purpose of our study was to assess the potential of a dynamic 3D contrast-enhanced MR angiographic sequence to characterize spinal vascular lesions and to identify their arterial feeders and venous drainage.**

METHODS: **A contrast-enhanced gradient-echo 3D pulse sequence providing angiographic information within 24 seconds was applied prospectively in 12 consecutive patients with a presumed spinal vascular lesion. The images were evaluated for visibility of the arterial feeder, and the results were compared with those of conventional angiography performed the next day.**

RESULTS: **The MR angiographic findings proved that the lesions were correctly characterized as spinal arteriovenous malformations (AVMs) (n = 6), spinal dural arteriovenous fistulas (AVFs) (n = 3), a hemangioblastoma (n = 1), a teratoma (n = 1), and a vertebral hemangioma (n = 1). The arterial feeder was visible in all six AVMs and in the hemangioblastoma, corresponding to conventional angiographic findings. In two of three spinal dural AVFs, an enlarged draining medullary vein was seen within the neural foramen, providing correct localization. The third fistula could not be seen owing to reduced image quality from motion artifacts.**

CONCLUSION: **Fast 3D contrast-enhanced MR angiography is a noninvasive technique with high accuracy in the characterization of spinal vascular disease. Visibility of the arterial pedicles corresponds well with that of digital subtraction angiography, facilitating the management of these patients.**

Vascular malformations of the spine and spinal cord are uncommon lesions. The prevalence, expressed as a percentage of the total number of spinal space-occupying lesions, is reported at 16% (1). The ratio of spinal to brain arteriovenous malformations (AVMs) ranges from 1:4 (2) to 1:8 (3). MR imaging is the primary method for noninvasive examination of patients with clinical evidence of a spinal cord lesion; however, MR findings are often nonspecific and may be due to spinal cord tumor, inflammation, or vascular disease. Because vascular malformations are a treatable cause of myelopathy, noninvasive techniques for depicting abnormal spinal vessels are desirable.

Accurate visualization of the angioarchitecture of these lesions and their correct classification are important for therapeutic planning and correct management of the patients. Preoperative, noninvasive identification and knowledge of the precise origin of the feeding arteries would potentially facilitate evaluation with catheter angiography by guiding selective arteriography to specific spinal levels, thus shortening the overall duration of the procedure.

These goals have been described in previous studies using time-of-flight (TOF) 3D (4) and phase-contrast 2D and 3D (5) techniques as well as dynamic contrast-enhanced MR imaging (6), with variable results. Alternatively, postmyelographic CT has been shown to be helpful in the differential diagnosis between spinal dural arteriovenous fistulas (AVFs) and intramedullary tumors by demonstrating enlarged veins on the cord surface (7).

Recently developed contrast-enhanced MR angiographic techniques have been successfully applied to the noninvasive evaluation of various vascular territories of the body (8, 9). These techniques simply depict the blood pool in a vessel instead of imaging complex flow. The ultrashort TE used al-

Received November 9, 1998; accepted after revision May 19, 1999.

From the Institute of Neuroradiology, University Hospital of Zurich, Frauenklinikstrasse 10, CH-8091 Zurich, Switzerland.

Address reprint requests to Spyros S. Kollias, MD.

lows fast acquisition times, permitting depiction of extended vascular territories within a single breath-hold, because the imaging plane can be oriented parallel to the vessels.

In the present study, we prospectively applied a fast contrast-enhanced 3D MR angiographic sequence in the examination of a series of patients with spinal vascular disease. Our purpose was to assess the potential of this technique to characterize these lesions correctly and to depict their feeding arteries and venous drainage before selective spinal arteriography and endovascular treatment.

Methods

Patients

Over a period of 8 months, 12 consecutive patients (nine male, three female; ages, 3 to 69 years; mean age, 42 years) were examined prospectively. The patients were referred to the section of interventional neuroradiology with symptoms suggestive of a spinal vascular lesion for further evaluation and potential endovascular treatment. The clinical signs were leg weakness (n = 10) in combination with bladder dysfunction (n = 4) or sensory changes (n = 3) (see Table). One patient had severe back pain owing to a vertebral body hemangioma and another patient had had a subarachnoid hemorrhage with a suspicious vascular lesion in the medulla oblongata. All subjects had an MR study, and, in all but the patient with the hemangioma, intra-arterial digital subtraction angiography (DSA) and endovascular treatment were performed the next day.

MR Imaging

All examinations were obtained on a clinical 1.5-T MR unit equipped with an ultrafast three-axis gradient system (maximum amplitude of 22 mT/m, rise time of 184 milliseconds, and slew rate of 120 mT/m per millisecond) using a standard spinal phased-array coil. The routine imaging protocol included the following sequences: sagittal T1-weighted (500/14/2 [TR/TE/excitations]; matrix, 256 × 192; field of view [FOV], 28 cm; thickness/gap, 3.5/0.6 mm), and sagittal and axial T2-weighted fast spin-echo (3500/105/4; echo train, 12; matrix, 256 × 192; sagittal: FOV, 28; thickness/gap, 3.5/0.6 mm; axial: FOV, 18 cm; thickness/gap, 5.0/1.5 mm). These series were evaluated for the presence of abnormal findings such as cord swelling, edema, and signal voids suggestive of abnormal vessels. On the basis of clinical neurologic deficits and the location of abnormalities on these images, contrast-enhanced MR angiography was performed. Initially, the circulation time was determined in each patient for optimization of contrast administration. Using a 2D radiofrequency (RF) spoiled gradient-echo sequence (TR/TE, 9.1/2.1; flip angle, 60°; thickness, 10 mm), multiple sequential images were obtained in a sagittal plane through the aorta during bolus injection of a low dose (2 mL) of contrast material followed by a saline flush. The bolus was started simultaneously with data acquisition and the circulation of contrast in the aorta was monitored every 1.3 seconds for a period of 53 seconds. The delay time between contrast injection and scan start used in the 3D contrast-enhanced sequence was calculated by the following equation: delay time = contrast appearance in the upper aorta for cervical or thoracic spine and lower aorta for lumbar spine − half the acquisition time of the 3D sequence. Thereafter, a commercially available contrast-enhanced fast gradient-echo 3D fat-suppressed pulse sequence was obtained in the coronal plane with the following parameters: TR/TE/excitations, 7/2.3/0.5; TI, 30; flip angle, 25°; receiver bandwidth, 31 kHz; and FOV, 280 mm (3/4 phase). Thirty-four, 2-mm-thick sections with a matrix of 256 × 192 (57 sections reconstructed to 512 × 384 after zero-fill interpolation) were acquired to cover the width of the spinal canal for the entire FOV. The acquisition time of the angiographic sequence was 24 seconds, which allowed collection of the data during breath-hold. Contrast material was injected intravenously through an 18-gauge angiocatheter placed into an antecubital vein. A dose of 0.2 mmol/kg was administered at a rate of 3 mL/s using an automated MR-compatible power injector. Sagittal and axial T1-weighted spin-echo sequences with fat saturation (500/14/3; matrix, 256 × 192; sagittal: FOV, 24 cm; thickness/gap, 3.5/0.6 mm; axial: FOV, 18 cm; thickness/gap, 5.0/1.5 mm) were then obtained to complete the diagnostic MR protocol. The time required to complete each patient's MR study was approximately 40 minutes.

MR Data Analysis

All MR data were transferred to a Sun workstation with commercially available software for further postprocessing and photography. A maximum-intensity pixel (MIP) projection algorithm was applied in all cases to create angiograms of the spinal vessels. Targeted views were used to eliminate overlapping structures, such as the kidneys, and subvolume reconstructions to differentiate between vessels on the anterior and posterior surface of the spinal cord. Additionally, the 3D data set was analyzed by thin multiplanar reformations. The postprocessing time was approximately 15 to 20 minutes for each patient. The analysis was performed jointly by two observers who evaluated the MR angiograms for the presence of vascular disease based on qualitative estimation of the number, size, and tortuosity of the identified intradural vessels; the visualization and localization of the arterial feeder; and the type and level of venous drainage. For categorization of the type of vascular disease, the classification of spinal cord vascular lesions as reported by Berenstein and Lasjaunias (10) was applied. This classification was used for its simplicity and its important clinical and prognostic significance. Hard copies of the MR angiograms were additionally reviewed by a third observer who subsequently performed the selective spinal arteriography and the interventional procedure. In all cases, the MR angiographic data were reviewed before intra-arterial angiography was performed. The only information available to the reviewers at the time of the MR examination were the clinical signs of the patient and the results of conventional contrast-enhanced MR imaging of the spine performed at different centers on 0.5-T or 1.5-T systems that had led to the suspicion of a spinal vascular malformation.

The findings were compared with those of digital subtraction angiography (DSA). Selective spinal arteriography was carried out using digital equipment. Biplane images of the spinal cord vascularization with 1024 × 1024 matrix resolution were obtained by selective catheterization of the intercostal and lumbar arteries.

Results

In 11 of 12 patients who were able to remain motionless and hold their breath for the 24-second acquisition time, good-quality contrast-enhanced 3D MR angiograms of the spinal vessels were obtained. Motion artifacts precipitated by severe back pain slightly decreased the image quality in one patient (case 7). There were no complications related to the bolus administration of contrast agent.

The MR angiographic diagnosis, visualization of the arterial feeder and its level, type of venous drainage, and extent of T2 signal abnormalities are summarized in the Table. Blinded interpretation of

MR angiographic findings and clinical symptoms in 12 patients with spinal cord vascular disease

Case	Age (y)/ Sex	Diagnosis/Location	Symptoms	Arterial Feeder, Level	Venous Drainage	T_2Hyperintensity Extension
1	58/M	SCAVM/L2 infraconal	Weakness of both legs, bladder dysfunction	Enlarged artery of Adamkievicz (radiculomedullary), T11	Enlarged posterior median vein	T6–conus
2	25/M	SCAVM/L1 conal	Weakness of both legs, bladder dysfunction	Enlarged artery of Adamkievicz (radiculomedullary), T11	Enlarged posterior median vein	T5–conus
3	26/F	SCAVM/C5	Weakness and parasthesia of left arm	Costocervical trunk (radiculomedullary)	Enlarged anterior and posterior median veins	C4–C6
4	19/F	SCAVM/medulla oblongata	Subarachnoidal hemorrhage	Left vertebral artery	Perimedullary veins	· · ·
5	36/F	Fistulous SCAVM/T11–L2	Weakness of both legs and pain	Enlarged radiculomedullary artery, T12	Descending varicose vein	T12–L1
6	24/M	SCAVF/L2, infraconal	Right leg weakness, sacral hypoesthesia, bladder dysfunction	Enlarged spinal anterior artery (radiculomedullary), T5	Descending varicose vein	T10–conus
7	69/M	SDAVF	Sensory loss and weakness of both legs, severe back pain	Not identified	Enlarged anterior median vein	T5–conus
8	67/M	SDAVF/T11	Weakness of both legs, bladder dysfunction	T11 (intervertebral foramen), T11/T12	Medullary vein from intervertebral foramen T11–T12 to enlarged posterior median vein	T7–conus
9	64/M	SDAVF/T6	Weakness of both legs	T6 (intervertebral foramen), T6–T7	Medullary vein from intervertebral foramen T6–T7 to enlarged posterior median vein	T8–conus
10	53/M	Hemangioblastoma with V on Hippel-Lindau disease, T12–L1	Sensory change and weakness of both legs	Enlarged artery of Adamkievicz (radiculomedullary), T11	Enlarged perimedullary veins	T10–conus
11	3/M	Presacral tumor with multiple AV shunts	Weakness of right leg	Multiple branches of internal iliac arteries	Epidural venous plexus	· · ·
12	60/M	Hemangioma, vertebral body T8	Back pain	No enlarged intradural artery visible	· · ·	· · ·

Note.—SCAVM indicates spinal cord arteriovenous malformation; SCAVF, spinal cord arteriovenous fistula; SDAVF, spinal cord dural arteriovenous fi stula.

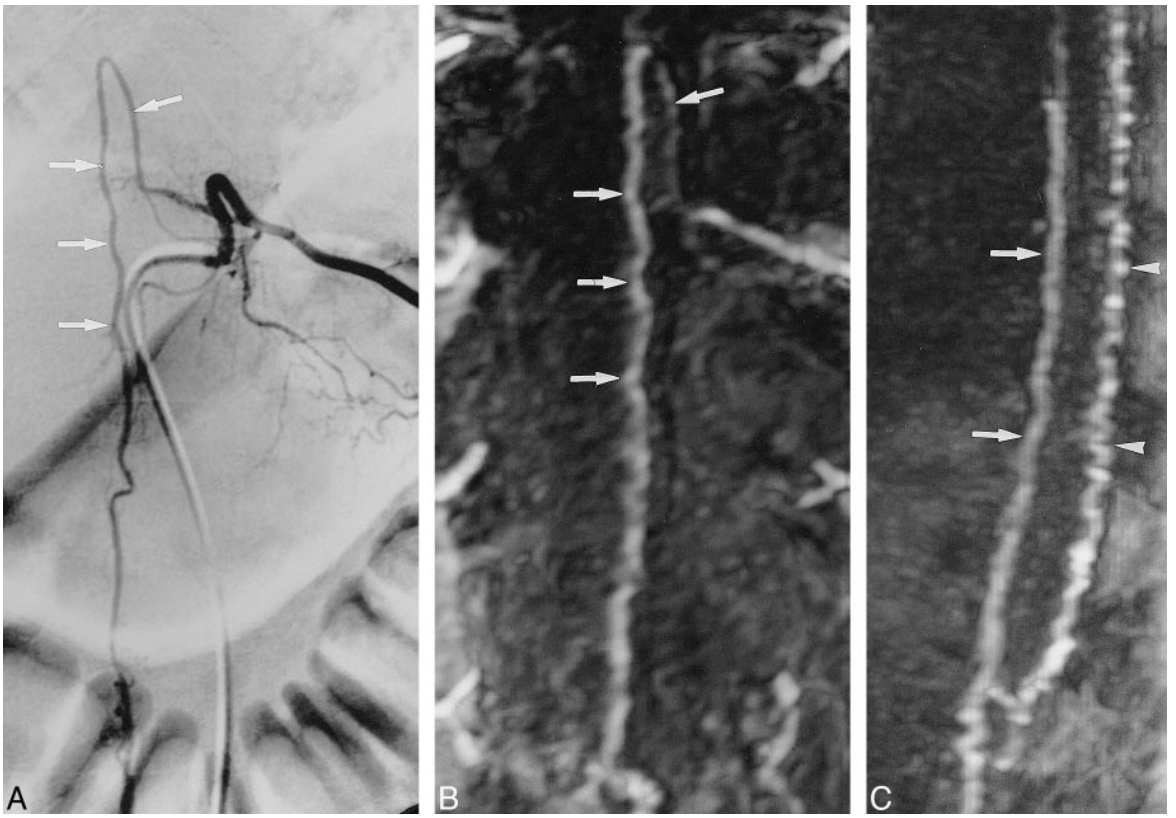

FIG 1. Infraconal spinal cord AVM (case 1).

A, DSA of a selective catheterization of the left intercostal artery at the T11 level shows an enlarged artery of Adamkiewicz (*arrows*).

B, Corresponding anteroposterior MIP projection of the MR angiogram shows similarity in the shape of the anterior midline vessel with that depicted in the arterial phase of the DSA (*arrows*).

C, Sagittal view shows the artery of Adamkiewicz on the anterior surface of the cord (*arrows*) and, dorsally, the enlarged draining posterior median vein (*arrowheads*).

the MR angiograms, before the DSA, reached a consensus among the three reviewers (100% agreement) regarding correct categorization of the type of vascular disease and visualization of the arterial supply and level of the feeder in all cases. In all six patients with spinal cord AVM (cases 1 through 4), spinal cord AVF (case 6), or a combination of the two (fistulous spinal cord AVM) (case 5), the main arterial feeder and the level of origin were identified on MR angiograms, and its location corresponded to that seen at DSA. A radiculomedullary supply was seen in five of the six patients, which corresponded to an enlarged artery of Adamkiewicz (n = 3) (Fig 1), an enlarged anterior spinal artery joining the parent fifth intercostal artery (n = 1), and an arterial feeder originating from the costocervical trunk (n = 1) (Fig 2). In the patient harboring a spinal cord AVM in the medulla oblongata, the arterial supply arose from the left vertebral artery. A distinction between radiculomedullary or radiculopial supply was not possible with MR angiography in this case. The type and extent of venous drainage were readily depicted in all these patients. A dilated vein with prominent tortuosity was seen in the patient with spinal cord AVF and in the one with spinal cord AVM with a fistulous component (Fig 3). The remaining cases showed slightly enlarged anterior or posterior median veins or both.

In two of the three spinal dural AVFs, the MR angiogram revealed the fistula itself in the neural foramen and a dilated medullary vein draining to an enlarged posterior median vein (Fig 4). In the third case with spinal dural AVF at the L1 level, proved by DSA, the quality of the MR angiograms was reduced by motion artifacts, and the level of the fistula could not be identified. Nevertheless, a spinal dural AVF was suspected because of an enlarged tortuous anterior median vein and a hyperintensity within the center of the cord on the T2-weighted images extending from the T5 level to the level of the conus.

Three patients with vascular spinal tumors were included in this study. In a patient with von Hippel-Lindau disease, a bilobular hemangioblastoma was identified at MR imaging. MR angiography depicted the arterial feeder, which consisted of an enlarged artery of Adamkiewicz, corresponding to DSA findings prior to embolization (Fig 5). A mass with multiple arteriovenous shunts fed by branches of the internal iliac arteries was found in a child with progressive weakness of the right leg. The intradural vessels were not enlarged, but early presentation of the epidural plexus was observed, ow-

FIG 2. Cervical spinal cord AVM (case 3).

A and *B,* DSA with simultaneous contrast injection in both subclavian arteries (*A*) and targeted anteroposterior MIP projection of the MR angiogram (*B*) show the main arterial feeder, which originates from the left costocervical trunk (*arrow*). The multicompartmental spinal cord AVM drains mainly into an enlarged posterior median vein (*arrowhead*).

FIG 3. Fistulous spinal cord AVM with a varicose venous drainage (case 5).

A and *B,* Both the late phase of selective DSA (*A*) and the MIP projection of the MR angiogram (*B*) show a tortuous, markedly enlarged draining vein (*arrowheads*). The arterial supply from the right 12th intercostal artery can be seen on MR angiogram in its proximal segment and at its sharp bend (*arrows*).

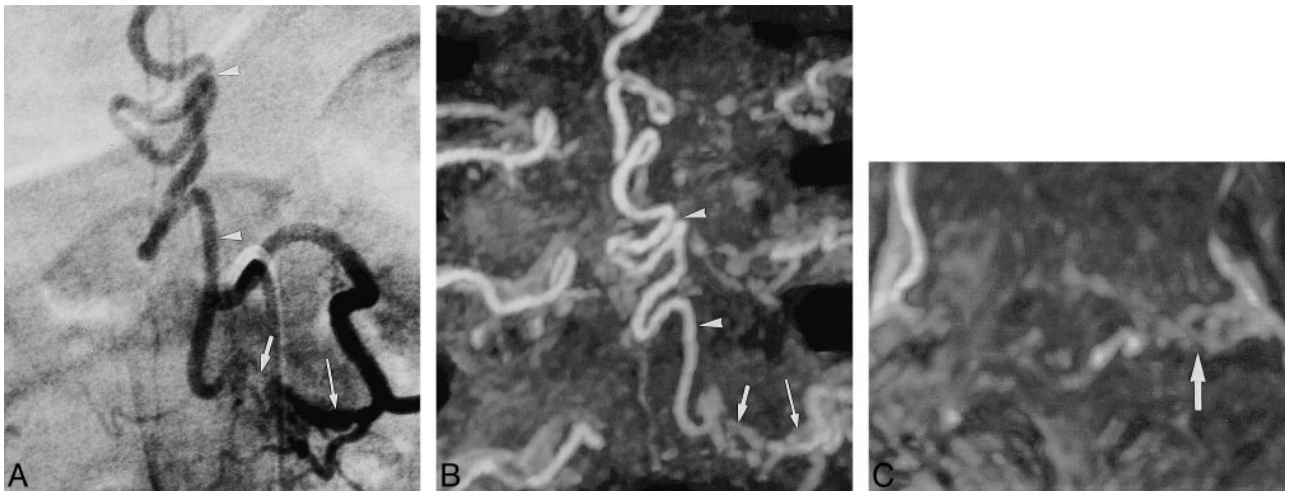

FIG 4. Spinal dural AVF at the left T11–T12 neural foramen (case 8).

A and *B,* Selective DSA (*A*) and anteroposterior MIP projection of MR angiogram (*B*) depict the fistula (*long arrow*) located at the T11–T12 neural foramen. An enlarged medullary vein (*short arrow*) draining the fistula to the tortuous, dilated posterior median vein (*arrowheads*) is clearly seen.

C, An axial targeted view from the MR angiographic data shows the location of the fistula (*arrow*) at the left T11–T12 neural foramen.

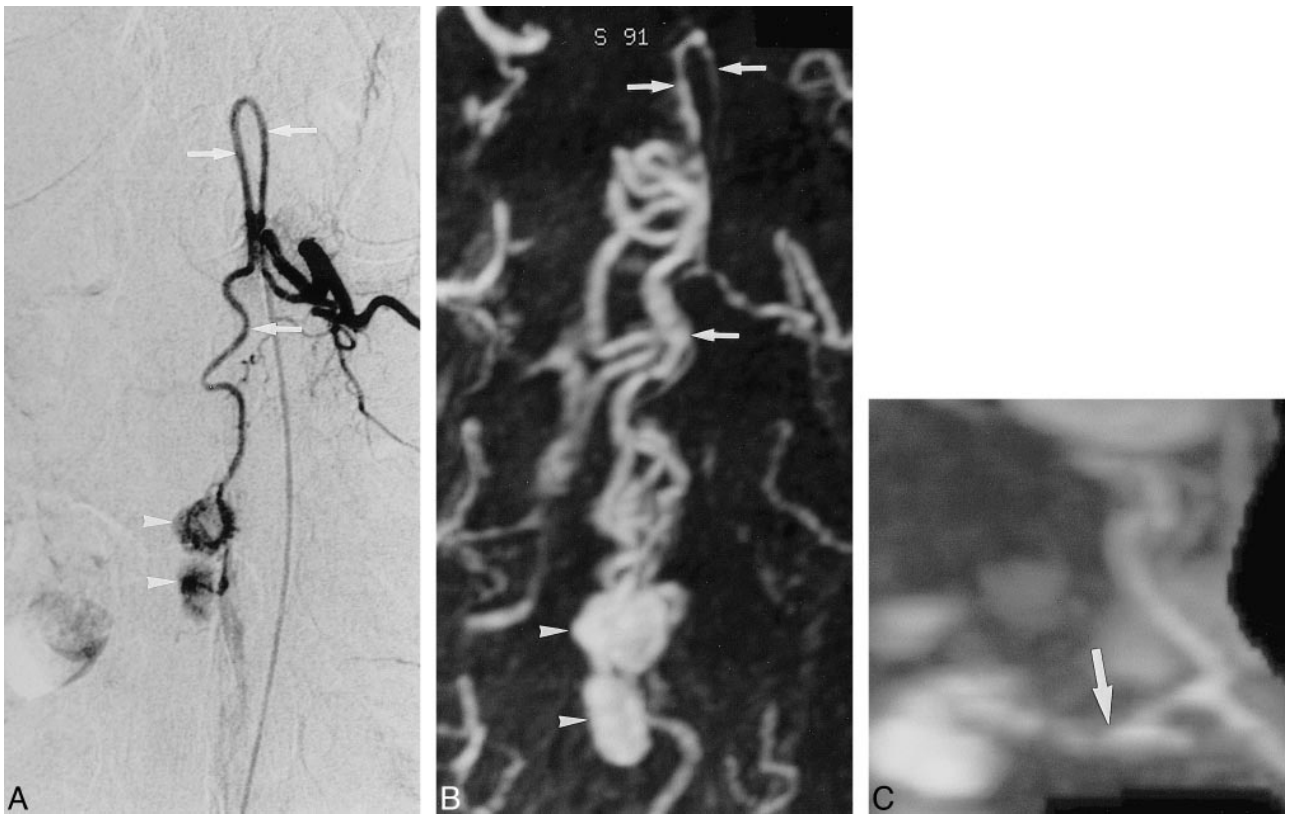

FIG 5. Bilobular hemangioblastoma in a patient with von Hippel-Lindau disease (case 10).

A and *B,* DSA with selective contrast administration into the left intercostal artery at T11 level (*A*) and the anteroposterior MIP projection (*B*) correspondingly show the two solid masses (*arrowheads*) fed by the enlarged artery of Adamkiewicz (*arrows*), which is partially obscured in the intradural course by enlarged draining perimedullary veins.

C, MIP axial targeted projection shows the arterial supply from the left T11 level (*arrow*).

ing to epidural drainage. The MR examination of this cooperative 3-year-old child was possible without anesthesia. He tolerated the MR angiographic sequence well, remaining motionless for its short acquisition time, and the resulting MR angiogram was of good quality. In the last patient with back pain without neurologic deficits, MR imaging revealed a vertebral body hemangioma. DSA was not performed in this case because the MR angiogram showed no enlarged intradural vessels. In nine of 12 patients, a confluent central hyperintensity of the cord was seen on the T2-weighted images. The extent of the signal abnormality ranged from two to nine vertebral segments, the largest being observed in patients with spinal dural AVFs (always including the conus medullaris) and in patients with spinal cord AVMs of the conal region. No T2 hyperintensity was visible in the patients with a vertebral hemangioma, a presacral tumor, or a small spinal cord AVM of the medulla oblongata.

Discussion

Vascular malformation of the spinal cord is a treatable cause of myelopathy. Therefore, correct categorization of the lesion and depiction of the arterial feeder are important to guide further diagnostic studies or endovascular treatment in these patients. Findings on MR images, such as signal abnormalities and cord enlargement, are often nonspecific and may result from a variety of pathologic processes, including spinal cord tumor, infection, and vascular disease. Moreover, an apparently normal MR study does not exclude a vascular lesion as the cause of clinical signs of myelopathy (11). Enlarged and abnormally tortuous intradural vessels in the subarachnoid space are often seen as serpentine areas of low signal intensity (flow voids) on T2-weighted images, guiding the diagnosis toward a vascular malformation or a vascular tumor (12, 13); however, the location of a suspected fistula or the level of the arterial feeder cannot be seen on these images. To improve the diagnostic accuracy of the MR examination, we performed fast contrast-enhanced 3D MR angiography in addition to conventional MR imaging. All nine vascular malformations were readily identified on MR angiograms and correctly categorized in relation to the DSA findings and according to the classification system of Berenstein and Lasjaunias (10), mainly differentiating between spinal dural AVFs and spinal cord AVMs.

Spinal dural AVFs represent an abnormal arteriovenous shunt that is not within the cord but in the surface of the dura, usually at the level of the intervertebral foramen. The fistula almost always drains intradurally by retrograde flow through a single medullary vein to the anterior or posterior median vein, resulting in engorgement of the coronal venous plexus (14). These lesions usually present after the fifth decade of life with a male predominance (15). Three male patients (age range, 64 to 69 years) with spinal dural AVFs were enrolled in our study. The diagnosis of spinal dural AVF was made on the basis of an enlarged, tortuous anterior or posterior median vein together with signal hyperintensity of the spinal cord on T2-weighted images extending from the conus over six to nine vertebral segments. In two cases, the fistula itself was directly visualized in the intervertebral foramen (Fig 4B). In one patient, the fistula was not depicted owing to reduced image quality caused by motion artifacts.

The other main group of spinal vascular malformations, the spinal cord AVMs, are supplied by medullary arteries (radiculomedullary or radiculopial) and drain through medullary veins. These lesions are on the surface of the spinal cord or are intramedullary in location. They may have a nidus, a direct fistula, or a combination of the two. The mean age at clinical presentation is the mid-20s, but close to 20% of the lesions are diagnosed in children under 16 years of age (16). In our group, the mean age at presentation was 31 years. Identification of the level of the main arterial feeder was possible in all six cases, which is helpful in planning endovascular treatment. In two cases, a fistulous component was identified by the depiction of a dominant tortuous medullary vein (Fig 3B). Three patients with vascular tumors were additionally included in this study. In one patient, with von Hippel-Lindau disease, a thoracic spinal hemangioblastoma was diagnosed. Spinal hemangioblastomas are usually intramedullary, involving the thoracic (61%) and the cervical (29%) cord (17). Based on the MR findings, this entity can be easily distinguished from spinal cord AVMs by the presence of a circumscribed solid mass. MR angiography identified the arterial supply of the tumor, which was fed by an enlarged artery of Adamkiewicz (Fig 5), although the intradural portion of the feeding artery was partially obscured by overlying enlarged perimedullary veins. Involvement of the intradural vessels was ruled out by MR angiography in the other two patients, with a vertebral body hemangioma and a presacral tumor, respectively.

Different techniques for identifying spinal vascular disease, especially spinal dural AVFs, have been applied in various studies. Dynamic contrast-enhanced MR imaging, analogous to cerebral blood pool and perfusion imaging, has been used to determine the approximate location (within one spinal level) of the fistula in patients with spinal dural AVFs (6). In the present study, susceptibility-induced signal changes after bolus injection of contrast material were first detected in the intradural veins (coronal venous plexus), which received the initial drainage from the fistula, allowing estimation of the approximate level in four of five cases. Abnormal intradural vessels associated with spinal vascular malformations have been routinely detected with both 2D and 3D phase-contrast angiography. Mascalchi et al (18) observed vascular ab-

normalities in five of six patients with spinal dural AVFs, and identified the arterial feeders in all three patients with spinal cord AVMs. Identification of the medullary vein draining the fistula was, however, only possible in two of six cases. More recently, the same authors (5) reported an improved ability to locate the fistula by additionally obtaining flow-direction information provided by the phase reconstruction of 2D acquisitions. By demonstrating diverging flow at the junction of the medullary vein draining the fistula and the coronal venous plexus, these investigators were able to obtain information as to the level of the fistula in nine of 11 patients. Using a contrast-enhanced 3D TOF sequence in the coronal or sagittal plane, Bowen et al (4) demonstrated the draining medullary vein in six of eight patients with spinal dural AVFs. Contrast administration was necessary to overcome spin saturation of flowing blood within the longitudinally oriented 3D slabs. Although the level of the fistula was indicated by depiction of the medullary draining vein, the fistula itself could not be seen directly. This technique illustrates the venous phase mainly because of the long acquisition time (11 minutes) of the sequence.

The fast 3D contrast-enhanced MR angiographic sequence used in the present study with the short acquisition time of 24 seconds focuses more on the arterial phase. Therefore, correct identification of the level of the arterial feeder prior to DSA was possible in all six patients with spinal cord AVMs and in the patient with hemangioblastoma. We emphasize, however, that knowledge of the normal spinal vascular anatomy is mandatory for correct interpretation of the MR angiograms in these patients. In a previous MR angiographic study of normal intradural vessels of the thoracolumbar spine using a 3D TOF contrast-enhanced technique (19), the only intradural vessels identified were the posterior and anterior median veins and the great medullary veins. Although no healthy control subjects were included in the present study, it seems that enlarged arterial structures associated with an AVM should be resolved using the present technique. The great anterior medullary artery (artery of Adamkiewicz) was not always depicted in its entire length, such as, for example, in case 5 (Fig 3); however, identification of its proximal segment and sharp bend and knowledge of normal spinal vascular anatomy led to the correct identification of the level of the feeder. Contrary to the indirect identification of the spinal dural AVF with dynamic contrast-enhanced MR imaging (6) and 2D or 3D phase-contrast (5, 18) and 3D TOF (4) techniques, the fistula could be seen directly in two of three patients in our study. The short acquisition time makes this sequence more feasible for less cooperative patients or children (eg, the 3-year-old patient examined without anesthesia). Contrast application was necessary in all previously applied spinal MR angiographic techniques (4–6). Correct timing of the contrast application facilitates the postprocessing workup by minimizing overlap of the intradural vessels and epidural plexus.

Although the sequence used in the present study depicts the arterial phase better than the 3D TOF technique does, further improvements are anticipated in distinguishing arteries from veins by the application of time-resolved contrast-enhanced MR angiographic sequences, with their faster acquisition times that promise better temporal resolution (9). The detectability of submillimeter-diameter intradural vessels could also be improved by the use of intravascular contrast agents that provide long-lasting excellent vascular enhancement, owing to their strong protein binding (20).

Conclusion

Our preliminary experience indicates that contrast-enhanced MR angiography is a useful sequence in the noninvasive workup of patients presenting with clinical signs of myelopathy. The technique provides additional information not afforded by conventional MR examination without significant prolongation of the scanning time or additional discomfort for the patient. Demonstration of the spinal vascular angioarchitecture helps in the correct characterization of these lesions, with prognostic and therapeutic significance. Direct visualization of the arterial feeder and the dural fistula provides useful information for planning endovascular treatment by guiding selective catheterization to specific spinal levels, thus reducing the amount of radiation received by the patients. Additionally, the technique, in combination with routine MR imaging, may be a promising alternative to DSA during follow-up of patients with spinal vascular disease.

References

1. Pia HW, Vogelsang H. **Diagnose und Therapie spinaler Angiome.** *Dtsch Z Nervenheilkd* 1965;187:74–96
2. Lombardi G, Migliavacca F. **Angiomas of the spinal cord.** *Br J Radiol* 1959;32:810–814
3. Bergstrand A, Hook O, Lidvall H. **Vertebral hemangiomas compressing the spinal cord.** *Acta Neurol Scand* 1963;39:59
4. Bowen BC, Fraser K, Kochan JP, Pattany PM, Green BA, Quencer RM. **Spinal dural arteriovenous fistulas: evaluation with MR angiography.** *AJNR Am J Neuroradiol* 1995;16:2029–2043
5. Mascalchi M, Quilici N, Ferrito G, et al. **Identification of the feeding arteries of spinal vascular lesions via phase-contrast MR angiography with three-dimensional acquisition and phase display.** *AJNR Am J Neuroradiol* 1997;18:351–358
6. Thorpe JW, Kendall BE, MacManus DG, McDonald WI, Miller DH. **Dynamic gadolinium-enhanced MRI in the detection of spinal arteriovenous malformations.** *Neuroradiology* 1994;36: 522–529
7. Kohno M, Takahashi H, Yagishita A. **Postmyelographic computerized tomographic scan in the differential diagnosis of radiculomeningeal arteriovenous malformation: technical note.** *Surg Neurol* 1997;47:68–71
8. Prince MR, Yucel EK, Kaufmann JA, et al. **Dynamic gadolinium enhanced 3D abdominal MR arteriography.** *J Magn Reson Imaging* 1993;3:877–881
9. Korosec FR, Frayne R, Grist TM, Mistretta CA. **Time-resolved contrast-enhanced 3D MR angiography.** *Magn Reson Med* 1996;36:345–351

10. Berenstein A, Lasjaunias P. **Spine and spinal cord vascular lesions.** In: Surgical Neuroangiography. New York: Springer; 1992; 5:1–5
11. Rosenblum DS, Myers SJ. **Dural spinal cord arteriovenous malformation.** *Arch Phys Med Rehab* 1991;72:233–236
12. Dormont D, Gelbert F, Assouline E, et al. **MR imaging of spinal arteriovenous malformations at 0.5 T: study of 34 cases.** *AJNR Am J Neuroradiol* 1988;9:833–838
13. Minami S, Sagoh T, Nishinmura K, et al. **Spinal arteriovenous malformations: MR imaging.** *Radiology* 1988;169:109
14. Kendall HE, Logue V. **Spinal epidural angiomatous malformations draining into intrathecal veins.** *Neuroradiology* 1977; 13:181
15. Symon L, Kuyama H, Kendall B. **Dural arteriovenous malformations of the spine: clinical features and surgical results in 55 cases.** *J Neurosurg* 1984;60:238–247
16. Yasargil MG, Symon L, Teddy PG. **Arteriovenous malformations of the spinal cord.** In: Symon L, ed. *Advances and Technical Standards in Neurosurgery*. Wien: Springer; 1984;11:61–102
17. Hurth M, Djindjian R, Houdart R, et al. **Hemangioblastomas intra-rachidiens.** *Neurochirurgie* 1975;21:1
18. Mascalchi M, Bianchi MC, Quilici N, et al. **MR angiography of spinal vascular malformations.** *AJNR Am J Neuroradiol* 1995; 16:289–297
19. Bowen BC, DePrima S, Pattany PM, Marcillo A, Madsen P, Quencer RM. **MR angiography of normal intradural vessels of the thoracolumbar spine.** *AJNR Am J Neuroradiol* 1996;17:483–494
20. Grist TM, Korosec FR, Peters DC, et al. **Steady-state and dynamic MR angiography with MS-325: initial experience in humans.** *Radiology* 1998;207:539–544